Chinese Journal of
POLYMER SCIENCE

RESEARCH ARTICLE

https://doi.org/10.1007/s10118-022-2741-1
Chinese J. Polym. Sci. **2022**, *40*, 1110–1119

A Glycosylated and Catechol-crosslinked ε-Polylysine Hydrogel: Simple Preparation and Excellent Wound Hemostasis and Healing Properties

Lin Teng[a,†], Zheng-Wei Shao[b,†], Yu-Shi He[c], Jia-Yu Lu[b*], De-Rong Zou[b], Chuan-Liang Feng[d], and Chang-Ming Dong[a*]

[a] *School of Chemistry and Chemical Engineering, Frontiers Science Center for Transformative Molecules, Shanghai Key Laboratory of Electrical Insulation and Thermal Aging, Shanghai Jiao Tong University, Shanghai 200240, China*
[b] *Department of Stomatology, Shanghai Jiao Tong University Affiliated Sixth People's Hospital, Shanghai Jiao Tong University, Shanghai 200233, China*
[c] *School of Chemistry and Chemical Engineering, Shanghai Electrochemical Energy Devices Research Center, Shanghai Jiao Tong University, Shanghai 200240, China*
[d] *School of Materials Science and Engineering, State Key Laboratory of Metal Matrix Composites, Shanghai Jiao Tong University, Shanghai 200240, China*

Electronic Supplementary Information

Abstract Commercial tissue adhesives have been widely applied in wound hemostats and dressings while enhancing the hemostasis and healing capabilities is challenging to meet clinical needs. Herein, we designed the glucose- and catechol-functionalized derivatives from commercial ε-polylysine (EPL) and prepared the hydrogels by simple amidation and catechol-crosslinking reactions, which have larger swelling ratios of 220%–240%, suitable microporous size of about 6–8 μm, and tissue adhesion strength of about 20–40 kPa. The hemolysis, cytotoxicity, and cellular double-staining assays indicate that those hydrogels had good biocompatibility and the H-3 hydrogel with higher glucose content gave a lower hemolysis ratio of 0.73%±0.14%. The blood-clotting index, blood cell attachment and adhesion studies showed those hydrogels had fast blood-coagulation, resulting in excellent hemostasis performance with a short hemostatic time of 38–46 s and less blood loss of 19%–34% in a liver hemorrhage model. A full-thickness rat-skin defect model further demonstrates that the H-3 hydrogel achieved fast wound healing with a wound closure of 70.0%±2.7% on postoperative day 7 and nearly full closure on day 14. Remarkably, the hydroproline level that denotes the collagen production reached a higher one of 7.24±0.55 μg/mg comparable to that in normal skins on day 14, evidencing the wound healing was close to completion in the H-3 treatment. Consequently, this work provides a simple method to construct a glycosylated and catechol-functionalized hydrogel platform from commercial EPL, holding translational potentials in wound hemostats and dressings.

Keywords Polylysine hydrogel; Glycosylation; Mussel-mimetic; Hemostasis; Wound dressing

Citation: Teng, L.; Shao, Z. W.; He, Y. S.; Lu, J. Y.; Zou, D. R.; Feng, C. L.; Dong, C. M. A glycosylated and catechol-crosslinked ε-polylysine hydrogel: simple preparation and excellent wound hemostasis and healing properties. *Chinese J. Polym. Sci.* **2022**, *40*, 1110–1119.

INTRODUCTION

Skin is the first line of defense to protect the body yet vulnerable, so billions of surgical hemostats and dressings are heavily needed to close wounds and traumas, stop bleeding, prevent microbial infections, and even boost wound healing.[1,2] At present, the commercial adhesives such as α-cyanoacrylate, fibrin glue, albumin bioglues, gelatinand poly(ethylene glycol) (PEG) derived ones (*e.g.*, Coseal and Duraseal) are available yet far from ideal in biocompatibility, tissue adhesion, hemostasis, and healing properties.[3–12] For instance, α-cyanoacrylates would cure exothermally to damage soft tissues along with the toxic degradation products.[3,4,9] Fibrin and albumin glues are biocompatible yet poorly adhesive and expensive while biocompatible PEG-based adhesives often lack of biological and adhesive properties.[4,7,10] Especially, it is difficult to functionalize the above materials for overcoming the drawbacks, boosting their properties, and endowing high values to meet clinical needs.[11–14]

Recently, the mussel foot proteins and their mimetic materials demonstrate strong and tunable adhesions to various organic and inorganic materials and surfaces due to multivalent interactions of their catechol and lysine groups.[1,4,8,15,16] Inspired by the chemical structures of mussel foot proteins, some emerging polypeptides including

* Corresponding authors, E-mail: angelinelu@sjtu.edu.cn (J.Y.L.)
E-mail: cmdong@sjtu.edu.cn (C.M.D.)
† These authors contributed equally to this work.
Special Issue: Biomedical Polymers
Received March 10, 2022; Accepted March 24, 2022; Published online June 24, 2022

commercial ε-polylysine (EPL), synthetic polylysine and polyglutamate, and other amino acid-derived ones have been designed for tissue adhesives and dressings.[4,8–10,17–20] For those purposes, several classes of polypeptide hydrogels with interpenetrating, double cross-linking, and/or self-assembling networks have made progresses although it is complicated to control the homogeneity and produce them on a large scale.[9,10,19] In contrast, commercial EPL with pendant amine groups becomes an important platform to construct various EPL-derived hydrogels for applications in wound adhesives and dressings.[8,21,22] For instance, Xu and Chi *et al*. reported a kind of dopamine-PEG-modified EPL hydrogel, which utilized PEG to enhance biocompatibility for wound healing.[8] Zhao and Yuan *et al*. constructed a kind of double-component hydrogels composed of catechol-modified EPL and aldehyde-dextran, which completely healed the full-thickness wounds within 20 days.[22] However, their complicated preparation and the heterogeneity in multi-component gelation hampered the advances of the EPL-based hydrogels. Therefore, it is imperative to find simple method to construct high-performance EPL-based hydrogels for would hemostats and dressings.

Inspired by biological functions and microstructures of extracellular matrixes (ECM) and mussel foot proteins, we reason that simple glycosylation and catechol modification would improve the biocompatibility and tissue adhesion of EPL.[10,23,24] Therefore, we designed the glucose-/catechol-modified EPL and prepared the hydrogels (*i.e.*, H-1, H-2, and H-3) with same catechol yet different glucose contents (Scheme S1, Tables S1 and S2 in the electronic supplementary information, ESI). As we know, the wound healing process generally experiences four stages: hemostasis, inflammation, proliferation, and tissue remodeling.[2,5,23,25] Therefore, the as-expected highly efficient hemostasis and less inflammation that might be achieved by the as-designed EPL-based hydrogels would benefit the latter stages.[9,10] In specific, the microstructures of the glucose-/catechol-modified EPL-based hydrogels would effectively seal wounds and accelerate hemostasis and healing process, in which the catechol groups mainly enhance the tissue adhesion and cross-link the EPL backbone to form an elastic network, the glucose groups boost biocompatibility and healing ability, and the microporous and moist 3D environment of the hydrogels would stop bleeding and play an antimicrobial barrier as wound dressings. Therefore, this work provides a simple method to fabricate a glycosylated and catechol-functionalized EPL-based hydrogel, which presents excellent would hemostasis and healing capabilities and holds translational potentials in wound hemostats and dressings.

EXPERIMENTAL

Materials

ε-Polylysine (EPL, M_w=3.5–5 kDa), horseradish peroxidase (HRP, 200 units/mg), and H_2O_2 (30 wt%) were purchased from Aladdin BioChem Technology. D-glucono-1,5-lactone (GDL) and 3,4-dihydroxyphenylpropionic acid (DA) were purchased from Sigma-Aldrich. *N*-hydroxysuccinimide (NHS) and 1-(3-dimethylaminopropyl)-3-ethylcarbodiimide hydrochloride (EDC·HCl) were purchased from TCI. Triethylamine (TEA), *N*,*N*-dimethylformamide (DMF), dimethyl sulfoxide (DMSO), and dichloromethane (DCM) were purchased locally. 3-(4,5-Dimethylthiazol-2-yl)-2,5-diphenyltetrazolium bromide (MTT) and the live/dead cell double staining kit were purchased from Sigma-Aldrich. LDH kit and hydroxyproline assay kit were purchased from Nanjing Jiancheng Bioengineering Institute (Nanjing, China).

Method

^{1}H-nuclear magnetic resonance (^{1}H-NMR, 400 MHz) spectroscopy was collected on a Varian Mercuryplus-400 spectrometer at room temperature. UV-Vis spectroscopy (UV-1800, Shanghai spectrum analysis, China) was employed to monitor the crosslinking reaction process, during which the mixed solution of polymer, HRP and H_2O_2 was diluted by a large amount of PBS and tested by a UV-Vis spectrophotometer. The hydrogel sample was quenched in liquid nitrogen and fully lyophilized to give the cryogel, which was sputtered by a thin layer of gold and then observed by a scanning electron microscope (SEM, Phenom Pro). Viscoelastic behaviors of hydrogels were tested by a parallel-plate rheometer (ARES-G2, TA) with a gap of 0.5 mm after they were incubated for 1 h at room temperature, during which the outer edge of the plate was sealed with silicon oil to prevent the moisture evaporation. The angular frequency sweeping was tested in the range of 1–100 rad/s and the strain was kept at 1%.

Synthesis of the Glucose-/Catechol-functionalized EPL (EPGD)

First, the glucose-functionalized EPL (*i.e.*, EPG) was synthesized according to previous reports.[10] EPL (1.28 g) was dissolved in DMSO (30 mL), and then TEA (1.4 mL) and different molar ratios of GDL were added to the solution. The reaction solution was vigorously stirred for 2 days at 50 °C and then precipitated in 150 mL of DCM. The precipitate was filtered and dialyzed (MWCO=1000) against deionized water for 2 days, and then lyophilized to give EPG with a yield of ~72%.

In the next step, EPGD was synthesized by the amidation reaction. Taking $EPG_{40}D_{20}$ (the subscript number denotes the degree of substitution in EPL) as an example, 91 mg of DA, 69 mg of NHS and 116 mg of EDC·HCl were dissolved in 3 mL of DMSO/DMF (*V*:*V*=3:1) and stirred overnight in an ice-water bath, and then 10 mL of EPG_{40} (50 mg/mL) in DMSO and 138 μL of TEA were added to the above solution, and the reaction continued for 2 days under N_2 atmosphere. The reaction solution was precipitated into DCM/diethyl ether (*V*:*V*=1:1), filtered, dialyzed (MWCO=1000) against deionized water for 24 h, and lyophilized to give a light yellow product of $EPG_{40}D_{20}$ (508 mg, 86% yield).

Preparation of the EPL-based Hydrogels

The hydrogels were fabricated by HRP catalyzed crosslinking of EPD or EPGD in the presence of H_2O_2. In a typical example, 24 mg of EPD_{20} was dissolved in 100 μL of PBS (pH 7.4, 10 mmol/L) and was then divided into two equal parts. 50 μL of EPD_{20} was mixed with 16 Units/mL of HRP, and another 50 μL of EPD_{20} was added 140 mmol/L of H_2O_2. The two resulting solutions were mixed at room temperature to form the hydrogels, as observed by a vial inverting method, in which the final concentration of polymer, HRP and H_2O_2 are 12 wt%, 8 Units/mL and 70 mmol/L, respectively. The hydrogels of EPD_{20}, $EPG_{20}D_{20}$ and $EPG_{40}D_{20}$

were named as H-1, H-2 and H-3, respectively.

Swelling Properties of the EPL-based Hydrogels

Cylindrical hydrogels (200 μL) with a diameter of about 1 cm were immersed in 10 mL of PBS (pH 7.4, 10 mmol/L) at 37 °C, and weighed after the water on the surfaces of hydrogels was wiped at regular intervals. The swelling ratios were calculated according to the following formula. Swelling ratio = $(W_t - W_0)/W_0 \times 100\%$, and both W_t and W_0 denote the weight at t time and initial weight of hydrogels. All the samples were repeated four times (n=4).

Adhesive Strength of the EPL-based Hydrogels to the Skin Tissue

Adhesive strength of hydrogels to the skin tissue was measured by a universal testing machine (50 N load cell, MTS, E43, USA) according to ASTM standard F2255-05. The porcine skin was cut into rectangular strips (3 cm × 1 cm) after removing excess fat, and 200 μL of hydrogels was adhered between two pieces of porcine skin with an overlapped area of 1 cm × 1 cm. The samples were tested at a speed of 5 cm/min after incubation for 12 h at 4 °C without any other wetting and pressing treatment (n = 5). Adhesive strength = F/A, in which F (N) represents the maximal force before peeling off the overlapped skin, and A (m^2) is the overlapped area.

In vitro Hemolysis of the EPL-based Hydrogels

First, 3.2% of sodium citrate anticoagulant was mixed with fresh rabbit blood to obtain the citrated rabbit blood (blood/anticoagulant = 9/1). Then 100 μL of hydrogel in 500 μL of citrated rabbit blood was vigorously shaken for 3 h at 37 °C. The blood was centrifuged at 4000 r/min for 10 min to collect the supernatant. The supernatant was diluted about 26 times with PBS and tested by a microplate reader. Hemolysis ratio = $(OD_{sample} - OD_{negative})/(OD_{positive} - OD_{negative}) \times 100\%$, optical density (OD) represents the absorbance at 540 nm. Both PBS and 1% Triton X-100 serve as the negative and positive control groups, respectively (n=3).

In vitro Cytocompatibility of the EPL-based Hydrogels

Briefly, 100 μL of hydrogel was prepared in a 96-well plate, incubated for 4 h at room temperature, washed for three times with PBS, and then sterilized by 254 nm UV for 15 min. The rabbit skin fibroblast cells were seeded on the surface of hydrogels with a cell density of 6000 cells per well. After incubation at 37 °C for 24 h and 48 h, respectively, the cells were treated by a MTT method, and the OD value at 490 nm was recorded by a microplate reader (n=5). In a similar way, 300 μL of hydrogel was incubated with the fibroblast cells in a 6-well plate, treated with a live/dead cell double staining kit, and observed by an inverted fluorescence microscope (BX51, Olympus).

Animals

SD rats (male, 200–250 g) and New Zealand white rabbits (male, 2–3 kg) were purchased from the Chinese Academy of Sciences (Shanghai, China). The animal experiments (approval #A2020097) were performed in accordance with the laboratory animals' guidelines approved by the Animal Ethics Committee of Shanghai Jiao Tong University.

Blood Clotting Index (BCI) of the EPL-based Hydrogels

$CaCl_2$ (0.1 mol/L, 1 mL) was mixed with 9 mL of citrated rabbit blood to activate blood. Activated blood (50 μL) was dropped onto the surface of hydrogels in a 96-well plate (100 μL per well), then 5 mL of deionized water was dropped to stop clotting, and dissolved the uncoagulated blood. The OD value at 540 nm was measured by a UV-Vis spectrometer. BCI = $(OD_{reference} - OD_{sample})/OD_{reference} \times 100\%$. 50 μL of activated blood in 5 mL of deionized water served as the reference (n=3).

Attachment Performance of the EPL-based Hydrogels

After 50 μL of citrated rabbit blood was added to the surface of hydrogels in a 96-well plate (100 μL/well) and incubated for 10 min at 37 °C, the unattached red blood cells (RBCs) were washed with PBS for three times, and then the hydrogel was immersed in 3 mL of deionized water to lyse the absorbed RBCs for 1 h. The OD value was recorded at 540 nm by a UV-Vis spectrometer. 50 μL of citrated rabbit blood in 3 mL of deionized water served as the reference group (n=4). Attachment percentage of RBCs = $OD_{sample}/OD_{reference} \times 100\%$.

As for the platelets' attachment, 50 μL of platelet rich plasma (PRP) from rabbit blood was dropped onto the surface of hydrogel and incubated for 10 min at 37 °C. The unattached platelets were washed with PBS for three times, and then the hydrogel was immersed in 1 mL of Triton X-100 solution (1%) for 1 h. According to the LDH kit introduction, the OD value at 490 nm was measured by a microplate reader. 50 μL of PRP served as the reference group (n=4), and the attachment percentage of platelets = $OD_{sample}/OD_{reference} \times 100\%$.

To observe RBCs and platelets adhesion to hydrogels, 100 μL of hydrogel was immersed in 1 mL of PBS, and 50 μL of rabbit blood or PRP was added, incubated for 3 min, and washed with PBS for three times to remove unattached rabbit blood or PRP. Subsequently, the hydrogel was soaked in 5 mL of glutaraldehyde (2.5%) for 2 h, respectively immersed in 50%, 60%, 70%, 80%, 90%, and 100% ethanol (5 mL) for 10 min, and observed by SEM.

In vivo Hemostasis of the EPL-based Hydrogels

A liver hemorrhage model of SD rat (male, 200–250 g) was used to access the hemostasis performance.[8,9] The anesthetized rats were dissected to expose their livers by laparotomy, and the liver hemorrhage model was created with a diameter of 5 mm. After filling hydrogels into the wounds, the blood loss within 2 min was collected with a pre-weighted filter paper and hemostatic time was recorded. The wound without treatment severed as the control (n=3). Relative blood loss (%) = $M_{sample}/M_{control} \times 100\%$, and M_{sample} and $M_{control}$ represent the blood loss of the sample and the control groups, respectively.

In vivo Wound Healing Performance of the EPL-based Hydrogels

A full-thickness skin defect model was established with round wounds (diameter = 1 cm) on the backs of the anesthetized rats (male, 200–250 g).[8–10] Then all hydrogels were *in situ* prepared with sterile PBS and filled the wounds, which were photographed at prescribed intervals and measured by Image J software. Wound closure (%) = $(S_0 - S_t)/S_0 \times 100\%$, and S_0 and S_t represent the area of wounds at zero and t time, respectively (n=5). On day 7 and 14, the tissues in wounds were excised, fixed in 4% paraformaldehyde, embedded in paraffin, cut into small pieces, stained with hematoxylin and eosin (H&E), and finally observed and photographed by an optical microscope

https://doi.org/10.1007/s10118-022-2741-1

(Lecia, DMLP). Inflammatory cells and the thickness of granulation and dermis/epidermis tissues were analyzed by randomly selecting five sites in each section (n=5×5). The tissues in wound sites were collected to measure the amount of hydroxyproline (μg/mg) by using a hydroxyproline assay kit (n=3).

RESULTS AND DISCUSSION

Preparation and Characterization of the EPL-based Hydrogels

According to Scheme S1 (in ESI), the EPL derivatives of glycosylated EPL (EPG), catechol-modified EPL (EPD), and glucose/catechol-modified EPL (EPGD) were easily prepared by a routine amidation chemistry, which was characterized by means of FTIR (Fig. S1 in ESI) and ^{1}H-NMR. As shown in ^{1}H-NMR spectra (Fig. 1A), the new proton peaks at 3.41–3.53, 3.92 and 4.20 ppm belong to the glucose residue in EPG, and those of catechols appear at 6.43, 6.60, 2.37 and 2.61 ppm in EPGD and EPD, and the degree of substitution is summarized in Table S1 (in ESI). The degree of substitution of the glucose and catechol groups was calculated by ^{1}H-NMR, and the results are summarized in Table S1 (in ESI). Note that the ^{1}H-NMR-determined degree of DA substitution is in good agreement with that calculated by UV-Vis spectroscopy.

Based on previous reports,[8–10,16,17,26] we reason that EPD and EPGD would form hydrogels in the presence of ferric chloride or horseradish peroxidase (HRP)/H_2O_2. Indeed, both EPD and EPGD formed hydrogels at a higher concentration of ≥23 wt% when added by ferric chloride (0.4 mmol/L, Fe^{3+}: DA=1:3) because dynamic cross-linking points enabled them gel; however, they gelled by chemical cross-linking at a lower concentration of 12 wt% in HRP/H_2O_2, as tested by an inverted tube method. From a practicable viewpoint, we preferred to study the gelation and properties of EPD and EPGD in HRP/H_2O_2. Considering the fast gelation caused heterogeneity and the remaining H_2O_2 induced cytotoxicity, we fabricated the EPL-based hydrogels in 70 mmol/L H_2O_2 and 8 Units/mL HRP at room temperature, and the hydrogels of EPD_{20}, $EPG_{20}D_{20}$ and $EPG_{40}D_{20}$ were respectively named as H-1, H-2 and H-3 for the following studies (Table S2 in ESI). To track the chemical cross-linking process (Fig. 1B, Scheme S2 in ESI), a model reaction of the EPD solution (0.2 mg/mL) in HRP/H_2O_2 was monitored in Fig. 1(C). The strong absorbance at 280 nm gradually redshifted to about 286 nm, indicating the formation of dicatechols' cross-linking points during the process of oxidation reaction.[10,27] Moreover, the rheological measurements demonstrate the EPL-based hydrogels maintain typical viscoelastic characteristics (Fig. 2A), *i.e.*, the mechanical modulus has an angular frequency independent correlation and the storage modulus (G') retains greater than loss modulus (G'') within ≤100 rad/s, ranging from 1.3 kPa to 1.9 kPa (Table S3 in ESI). These above data evidence that the HRP-catalyzed oxidative reaction of catechol groups made EPD

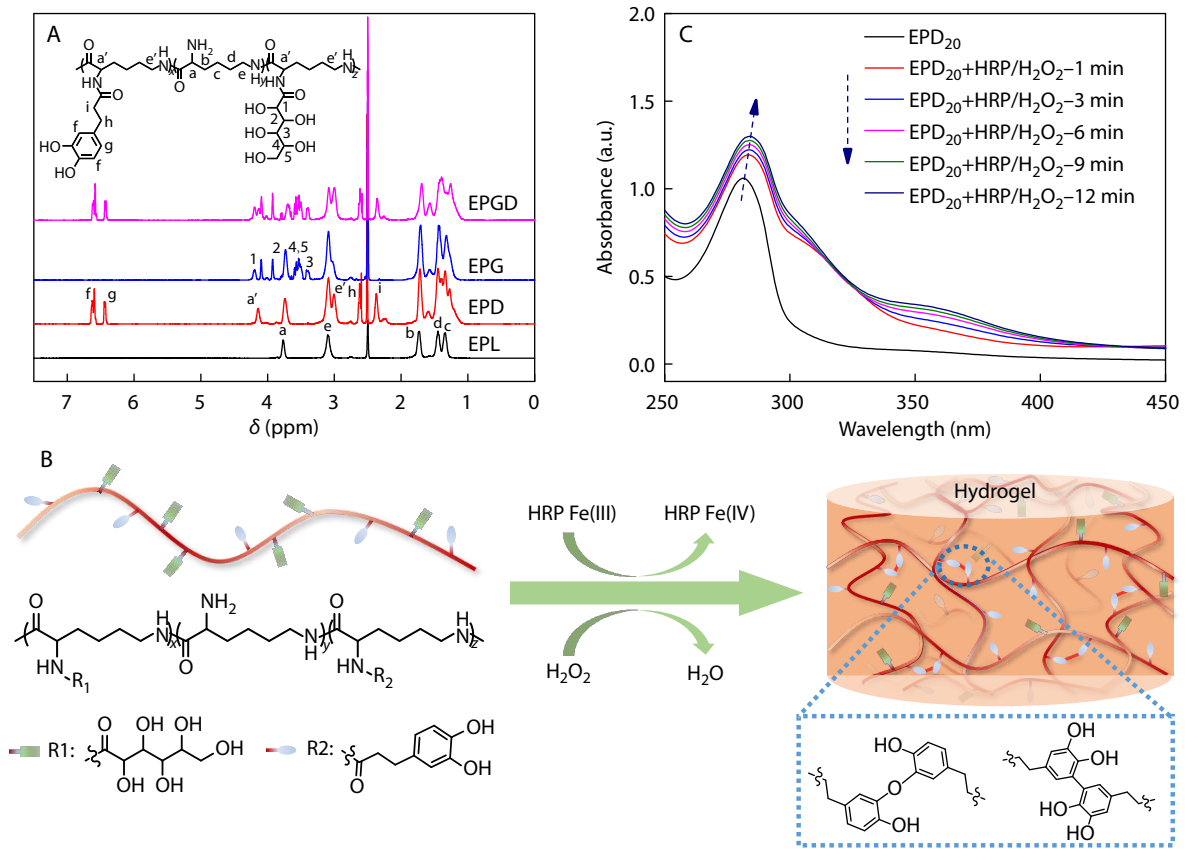

Fig. 1 (A) ^{1}H-NMR spectra (DMSO-d_6) of various EPL derivatives, (B) scheme for the catechol cross-linking catalyzed by HRP/H_2O_2, and (C) the time-evolved UV-Vis spectra of EPD_{20} (0.2 mg/mL) in the presence of HRP/H_2O_2 at room temperature.

https://doi.org/10.1007/s10118-022-2741-1

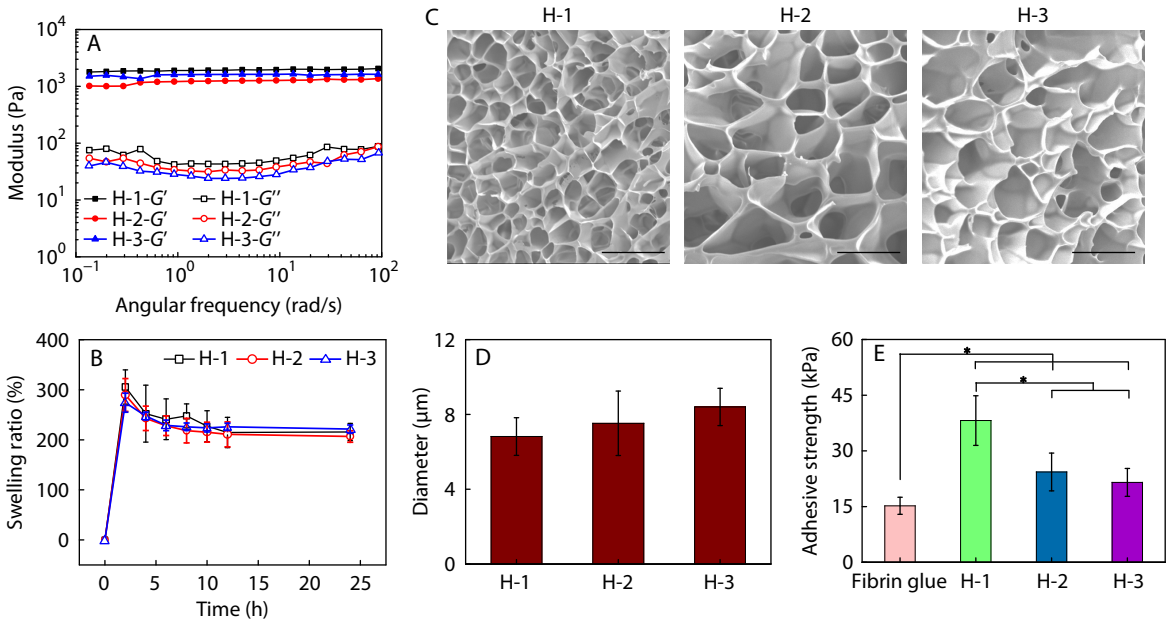

Fig. 2 Physicochemical properties of the EPL-based hydrogels: (A) rheological measurements, (B) swelling ratio dependent on time (n=4), (C) SEM images (scale bar=10 μm) and (D) pore sizes of the lyophilized hydrogels (*i.e.*, cryogels), and (E) tissue adhesive strength (n=5, *p<0.05).

and/or EPGD form the respective hydrogels. In addition, the gelation process of those EPL-based hydrogels is fast enough to be suitable for practical usage as the gelation time is less than about 50 s.

Whether do the hydrogels quickly absorb blood and wound exudate is a key factor for wound hemostasis and dressings.[28–31] To mimic this process, the swelling behaviors of the hydrogels were measured in PBS (10 mmol/L, pH 7.4) at 37 °C (Fig. 2B). Those hydrogels could quickly absorb water and reached an equilibrium swelling ratio of 220%–240% within about 4 h, indicating that the hydrogels had tight cross-linking networks to constrain water. The fast swelling behavior also implies that they should have porous microstructures. Note that the heterogeneous lower-cross-linked portion in the hydrogels might be dissolved to induce mass reduction as the amide bond should not be degraded in PBS buffer at 37 °C within a few days. As observed by SEM, the lyophilized hydrogels (*i.e.*, cryogels) showed microporous structures with average pore sizes of 6.8–8.4 μm (Figs. 2C and 2D). As the pore sizes are to some extent larger than 2–5 μm of blood cells and platelets, enabling the hydrogels beneficial for hemostasis. Moreover, the surface adhesion to wet tissues enables the hydrogels seal the wounds.[32–35] As measured by a lap-shear method, the adhesive strength of H-1 (EPD_{20} hydrogel), H-2 ($EPG_{20}D_{20}$ hydrogel), and H-3 ($EPG_{40}D_{20}$ hydrogel) is 38.2, 24.3 and 21.1 kPa, respectively (Fig. 2E). H-2 and H-3 give a relatively decreased adhesive strength than H-1 yet higher than 15.2 kPa of fibrin glue. H-2 and H-3 have the same catechol content yet lower lysine percentage than H-1, so the deceased adhesion can be attributed to the gradual glycosylation in H-2 and H-3. This indicates that the catechol and amine groups in the hydrogels played major roles in the surface adhesion while the multiple electrostatic, cation-π, and π-π stacking interactions among the hydrogels and wet tissues might enhance the adhesive strength more than the hydrogen bonding of glucose residues with tissues.[8,15,36] In all, the glycosylated and catechol-functionalized EPL-based hydrogels can be easily prepared by a general amidation modification of commercial EPL followed by an HRP enzyme-catalyzed catechol cross-linking, which have larger swelling ratio, microporous size, and wet surface adhesion for the application in wound dressings.

In vitro Biocompatibility and Blood Coagulation of the EPL-based Hydrogels

The biocompatibility of hydrogels is a prerequisite property when used for wound dressings and implants.[17,37] The blood compatibility (*i.e.*, hemocompatibility) was first tested by a common hemolysis method1.[9,10,17] As shown in Fig. 3(A), the blood supernatant in the EPL-based hydrogels looks light yellow similar to that in fibrin glue compared to that in Triton-X 100, implying a good hemocompatibility. The hemolysis ratios of H-1, H-2, and H-3 are heavily lower than the ASTM standard (*i.e.*, <5%), indicating a prominent hemocompatibility (Fig. 3B and Table S4 in ESI). Note that H-3 has a hemolysis ratio of 0.73%±0.14% close to that of fibrin glue, but lower than 1.21%±0.18% of H-1 and 0.87%±0.20% of H-2, which evidenced that the simple glucose modification can effectively improve the hemocompatibility of the EPLy-based hydrogels. Furthermore, the cytotoxicity of the hydrogels was accessed by a contact method,[8–10] in which the skin fibroblast cells were planted on the surface of the hydrogels for 24 h and 48 h, respectively. As shown in Fig. 3(C), the optical density (OD) value for H-3 is higher than that for H-1 after incubation (p<0.001), indicating the glycosylated EPL-based hydrogels have less cytotoxicity than non-glycosylated one. In addition, a live/dead cell double staining technique was employed to observe the cellular growth on the surface of hydrogels (Fig. 3D). The fibroblast cells grow better on H-3 than H-1, which is in accordance with the cytotoxicity result. In all, *in vitro* hemolysis and cytotoxicity evidence that a simple glycosylation can effectively improve the biocompatibility of commercial EPL derived hydrogels.[10,38–40]

Given the above-mentioned good water absorption, por-

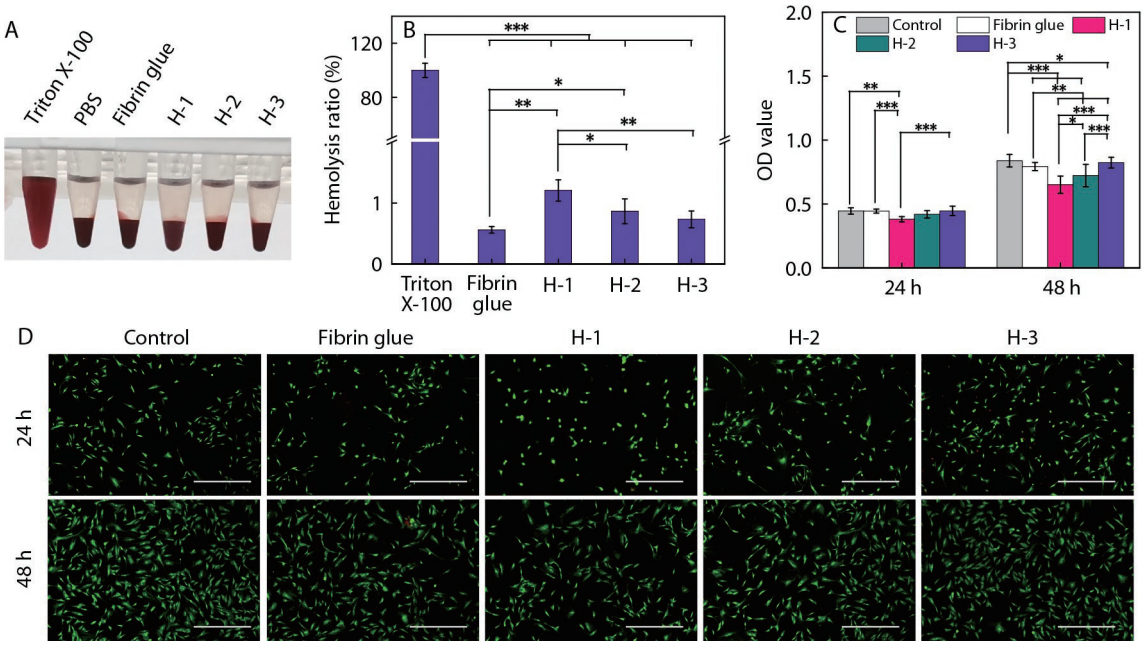

Fig. 3 *In vitro* biocompatibility of the EPL-based hydrogels. (A, B) Hemolysis properties (n=3), (C) cytotoxicity (n=5, *p<0.05, **p<0.01, ***p<0.001), (D) fluorescence microscope photographs of the fibroblasts cultured on the surfaces of hydrogels for 24 and 48 h (scale bar=200 μm).

ous microstructure, tissue adhesion, and *in vitro* biocompatibility, the EPL-based hydrogels are expected to be a hemostat *in vitro*. The blood-clotting index (BCI) is often used to characterize a hemostat, and a small BCI value denotes fast blood coagulation.[31,37,41] As shown in Fig. 4(A), the EPL-based hydrogels present faster blood coagulation performance than the positive control of fibrin glue while no obvious variance existed in H-1, H-2, and H-3. The procoagulant performance of hydrogels is related to the adsorption of blood cells including RBCs and platelets. As shown in Figs. 4(B) and 4(C) and Table S4 (in ESI), those EPL-based hydrogels adsorb more RBCs and platelets than the fibrin glue, and the absorbing amount increased by 43%–50% and 40%–45%, respectively. However, the attachment performance of RBCs and platelets has no statistical difference among H-1, H-2 and H-3 (p>0.05) because of their similar porous microstructures, which is consistent with the BCI results. This result also suggests that the microstructure of hydrogels has a great impact on the adhesion to blood cells, which is consistent with previous reports.[9,10,41] As further observed by SEM in Fig. 4(D), the RBCs and platelets adhering on the surface of hydrogels retain similar morphology to those in the fibrin glue while the platelets on the hydrogels were activated to secret some pseudopodia for accelerating blood coagulation.[41] These results indicate that the EPL-based hydrogels might mainly activate the platelets, playing a key role for coagulation than the RBCs during the hemostasis process.[10,31,41]

In vivo Hemostasis and Wound Healing of the EPL-based Hydrogels

Encouraged by the good blood coagulation of the EPL-based hydrogels *in vitro*, we further tested *in vivo* hemostasis by using the rat liver hemorrhage model.[9,31,37,41] As shown in Fig. 5(A), a larger amount of blood left on filter paper in the control and the fibrin glue than that in the EPL-based hydrogels. In specific, the fibrin glue stopped bleeding within 69±11 s, giving a larger blood loss of 44%±10% while those hydrogels showed a shorter hemostatic time of 38–46 s and less blood loss (19%–34%), as shown in Figs. 5(B) and 5(C) and Table S5 (in ESI). Those data demonstrate that the EPL-based hydrogels outperformed the fibrin glue. As a note, H-3 has an increase in blood loss and hemostasis time than H-1, which is due to the fact that the latter has stronger tissue adhesive strength (38.2 kPa) than the former (21.1 kPa) despite similar microporous size.[10,13,14]

The wound healing process usually experiences four stages: hemostasis, inflammation, proliferation and remodeling.[10,23,37] Therefore, the good hemostatic performance and biocompatibility enable the EPL-based hydrogels potential for wound dressings, which was accessed by a full-thickness rat skin defect model.[8–10] As shown in Figs. 6(A)–6(C), the wounds in the fibrin glue and the hydrogel groups heal to a close completion on the 14th day compared to large ones in the PBS group. In specific, the H-3 with higher glucose content shows a fast healing rate with a wound closure of 31.6%±3.0% and 70.0%±2.7% on postoperative day 3 and 7 (p<0.05), which is better than that in fibrin glue and H-1 (Table S6 in ESI). These results indicate that the higher glycosylation accelerated the wound healing although H-1 had better *in vivo* hemostasis than H-3, which is due to the improved biocompatibility of glycosylated EPL hydrogels. The above results also evidence that the biocompatibility would play a key role for wound healing when the hydrogels have a comparative hemostasis performance with the fibrin glue, which agreed well with previous studies.[6,9,10,14]

In order to further decipher the wound healing process, the dissected wounds were stained with hematoxylin and eosin (H&E). During the healing process, the new granulation tissue thickened on postoperative day 7 (Fig. 6D), and mainly turned into dermis on day 14 for the groups treated by fibrin glue and the EPL-based hydrogels, indicating that the wound heal-

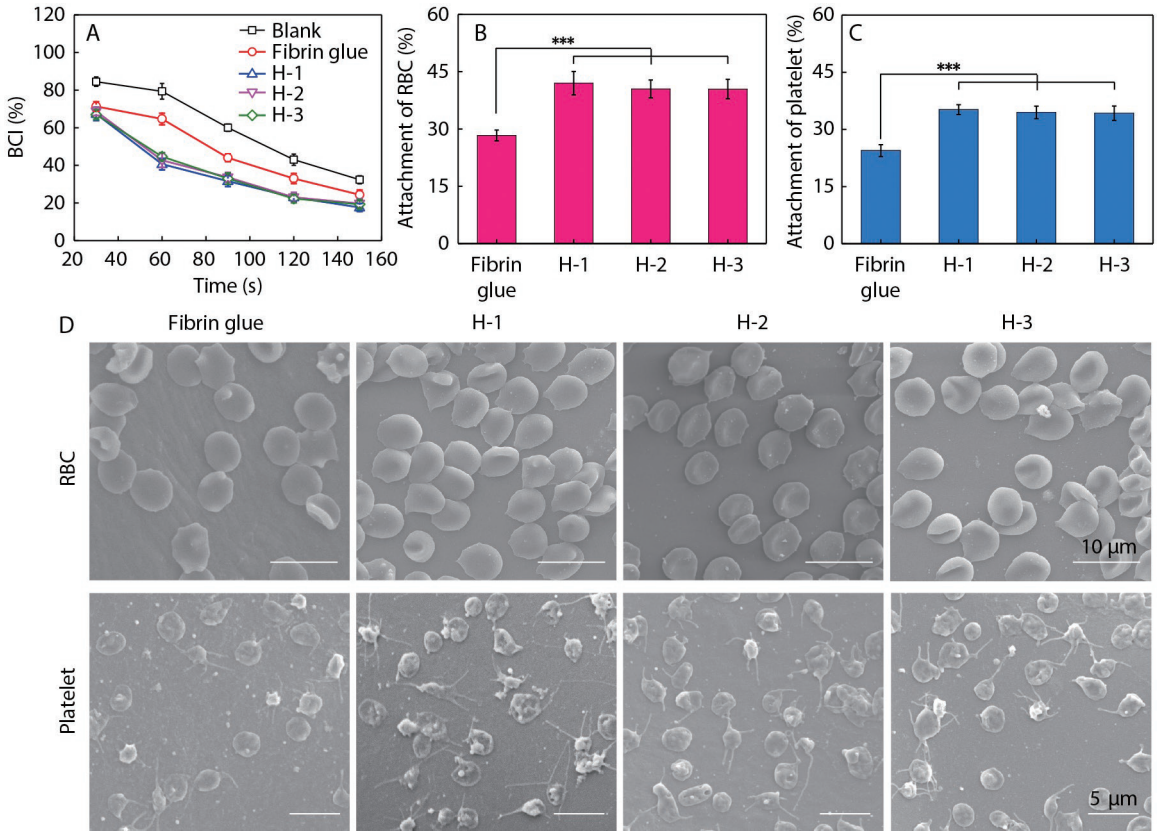

Fig. 4 The blood coagulation assays of the EPL-based hydrogels. (A) Blood clotting index (BCI, n=3), (B, C) the attachment performance (n=4, *p<0.05, **p<0.01, ***p<0.001), and (D) the SEM images for RBCs and platelets adhering to the hydrogels.

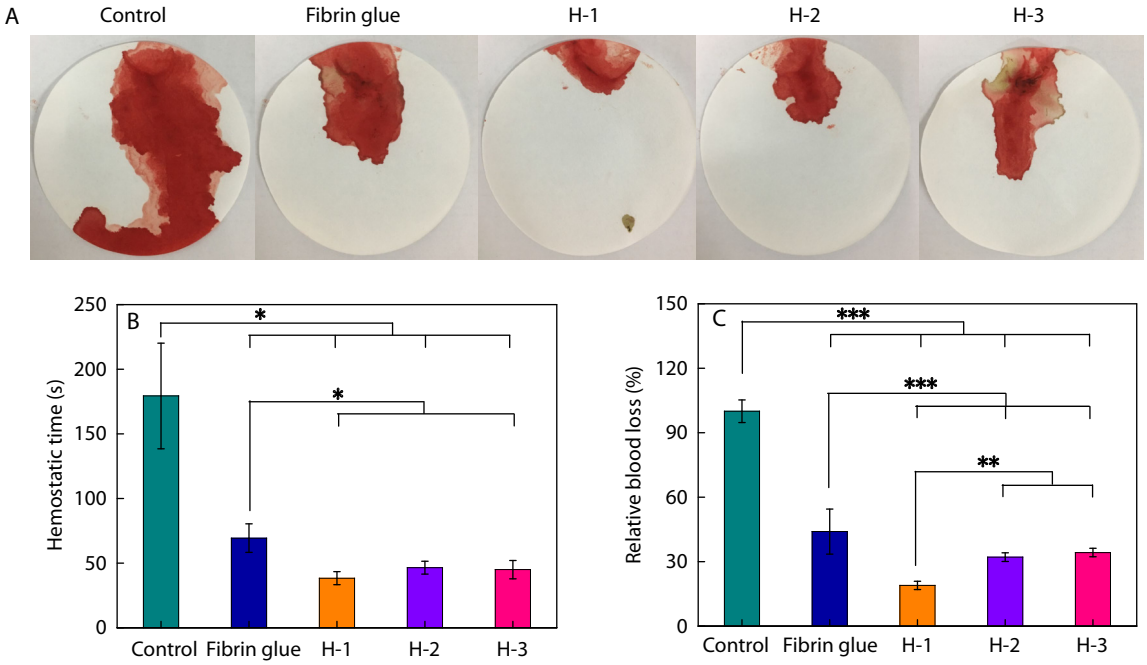

Fig. 5 *In vivo* hemostatic performance of the EPL-based hydrogels. (A) Representative photos of liver bleeding, (B) hemostatic time, and (C) relative blood loss of a liver hemorrhage model (n=3).

ing entered the remodeling stage; in contrast, main granulation tissue existed in the PBS group, suggesting the healing in a proliferation stage. As shown in Figs. 6(E) and 6(F), H-3 has a lower inflammatory cell infiltration of 21%±2% than those for both H-1 and fibrin glue groups and a thicker dermis of 1561±51 μm on the 14th day, showing an optimal wound

https://doi.org/10.1007/s10118-022-2741-1

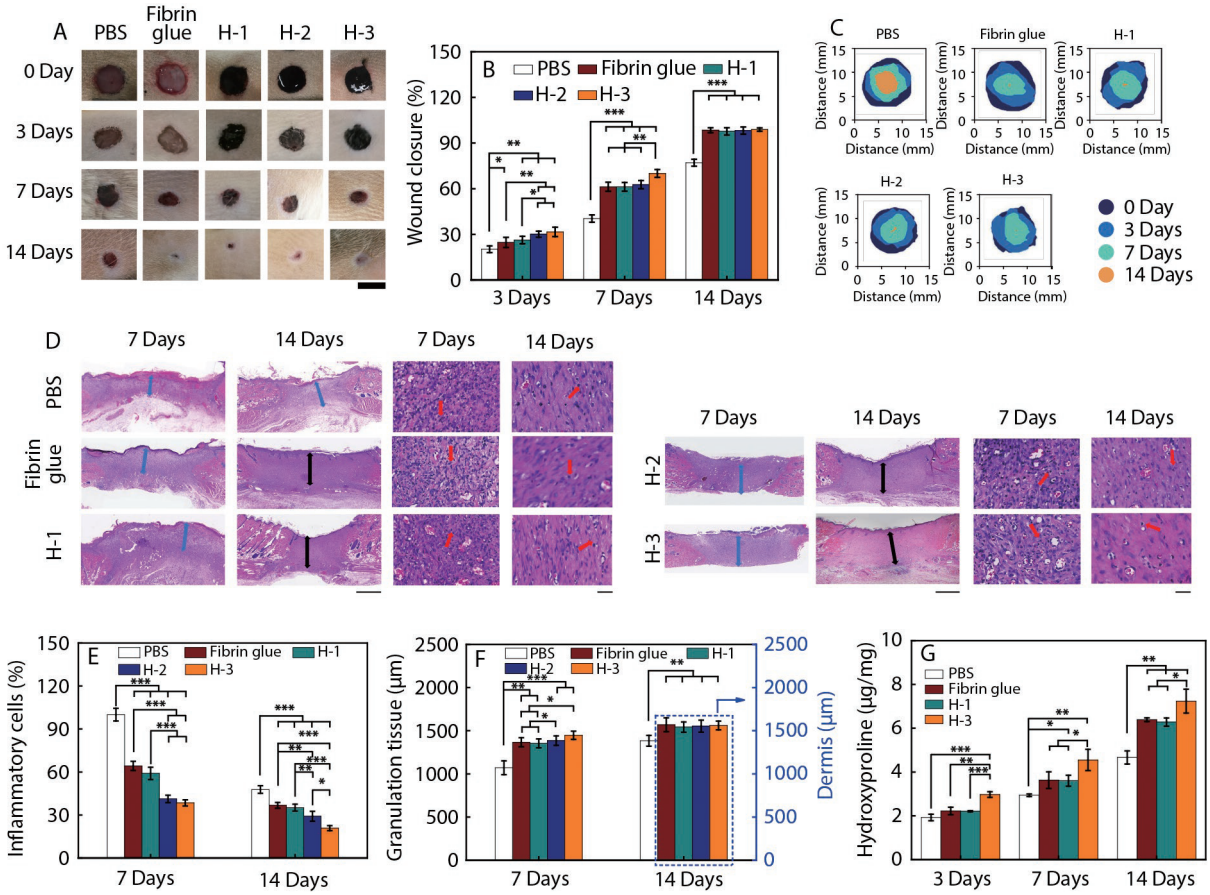

Fig. 6 *In vivo* wound healing performance of the EPL-based hydrogels. (A) Photographs, (B) wound closure, and (C) schematic diagrams of wounds at different time (n=5 and scale bar=1 cm), (D) the low (scale bar=100 μm) and high (scale bar=20 μm) magnified H&E images of the wounds on day 7 and 14 (blue arrow: granulation tissue, black arrow: dermis, red arrow: inflammatory cell), (E) inflammatory cells (n=5×5), (F) the thickness of granulation and dermis (n=5×5), and (G) the hydroxyproline level in wounds on day 3, 7, and 14 (n=3).

healing performance. In addition, a few hair follicles regenerated in the dermis for the H-3 group compared to the H-1 group (Table S6 in ESI).

Hydroxyproline is a unique amino acid in collagen with a constant percentage of about 13 wt%,[31] which is a common biomarker to denote the collagen production in tissues. The healed tissues on day 3, 7, and 14 were harvested and measured by a hydroxyproline kit and the hydroxyproline content gradually increased over the healing time (Fig. 6G). Notably, the hydroxyproline for the H-3 group on day 14 reaches up to 7.24±0.55 μg/mg higher than 6.39±0.08 μg/mg for fibrin glue and 6.28±0.19 μg/mg for H-1 groups (p<0.05). This was comparable to 6.90±0.48 μg/mg in normal rat skins as we measured, further evidencing that the wound healing should be close to completion in the H-3 group. Collectively, the above data demonstrate that the glucose-/catechol-functionalized EPL hydrogel of H-3 presented optimal and better wound healing capability than fibrin glue, holding clinical transition potential in wound dressings.

CONCLUSIONS

In summary, we put forward a facile method to construct the glucose-/catechol-functionalized EPL-based hydrogels. By increasing the glucose percentage, the biocompatibility of those hydrogels could be improved with H-3 giving a lower hemolysis ratio of 0.73%±0.14%. The liver hemorrhage model indicates that those hydrogels presented excellent hemostasis performance with shorter hemostatic time and less blood loss due to their larger swelling ratio, microporous size, and wet surface adhesion. The histological assays of H&E staining and hydroproline kit evidence that the H-3 hydrogel achieved better wound healing performance on a full-thickness rat-skin defect model within 14 days, and the hydroproline level in the H-3 treatment group is comparable to that in normal skins. So, the cooperative glycosylation and catechol-modification make commercial EPL suitable for constructing high performance wound hemostats and dressings with potential transition applications.

NOTES

The authors declare no competing financial interest.

Electronic Supplementary Information

Electronic supplementary information (ESI) is available free of charge in the online version of this article at http://doi.org/10.1007/s10118-022-2741-1.

ACKNOWLEDGMENTS

This work was financially supported by National Key Research and Development Project of China (No. 2021YFB4001101), the National Natural Science Foundation (NSFC) of China (No. 22075176), Natural Science Foundation of Shanghai (No. 22ZR1429200), and NSFC projects (Nos. 51833006, 82071160, 81870806 and 81974152).

REFERENCES

1 Zhao, Y.; Song, S.; Ren, X.; Zhang, J.; Lin, Q.; Zhao, Y. Supramolecular adhesive hydrogels for tissue engineering applications. *Chem. Rev.* **2022,** DOI: 10.1021/acs.chemrev.1c00815.
2 Zuo, X. L.; Wang, S. F.; Le, X. X.; Lu, W.; Chen, T. Self-healing polymeric hydrogels: toward multifunctional soft smart materials. *Chinese J. Polym. Sci.* **2021**, *39*, 1262–1280.
3 Chen, K.; Wu, Z.; Liu, Y.; Yuan, Y.; Liu, C. Injectable double-crosslinked adhesive hydrogels with high mechanical resilience and effective energy dissipation for joint wound treatment. *Adv. Funct. Mater.* **2022,** DOI: 10.1002/adfm.202109687.
4 Pourshahrestani, S.; Zeimaran, E.; Kadri, N. A.; Mutlu, N.; Boccaccini, A. R. Polymeric hydrogel systems as emerging biomaterial platforms to enable hemostasis and wound healing. *Adv. Healthc. Mater.* **2020**, *9*, e2000905.
5 Nam, S.; Mooney, D. Polymeric tissue adhesives. *Chem. Rev.* **2021**, *121*, 11336–11384.
6 Zhang, K.; Chen, X.; Xue, Y.; Lin, J.; Liang, X.; Zhang, J.; Zhang, J.; Chen, G.; Cai, C.; Liu, J. Tough hydrogel bioadhesives for sutureless wound sealing, hemostasis and biointerfaces. *Adv. Funct. Mater.* **2022,** DOI: 10.1002/adfm.202111465.
7 Yuk, H.; Varela, C. E.; Nabzdyk, C. S.; Mao, X.; Padera, R. F.; Roche, E. T.; Zhao, X. Dry double-sided tape for adhesion of wet tissues and devices. *Nature* **2019**, *575*, 169–174.
8 Wang, R.; Li, J.; Chen, W.; Xu, T.; Yun, S.; Xu, Z.; Xu, Z.; Sato, T.; Chi, B.; Xu, H. A biomimetic mussel-inspired ε-poly-*l*-lysine hydrogel with robust tissue-anchor and anti-infection capacity. *Adv. Funct. Mater.* **2017**, *27*, 1604894.
9 Bai, Q.; Teng, L.; Zhang, X.; Dong, C. M. Multifunctional single-component polypeptide hydrogels: the gelation mechanism, superior biocompatibility, high performance hemostasis, and scarless wound healing. *Adv. Healthc. Mater.* **2022**, *11*, e2101809.
10 Teng, L.; Shao, Z.; Bai, Q.; Zhang, X.; He, Y. S.; Lu, J.; Zou, D.; Feng, C.; Dong, C. M. Biomimetic glycopolypeptide hydrogels with tunable adhesion and microporous structure for fast hemostasis and highly efficient wound healing. *Adv. Funct. Mater.* **2021**, *31*, 2105628.
11 Wu, S. J.; Yuk, H.; Wu, J.; Nabzdyk, C. S.; Zhao, X. A Multifunctional origami patch for minimally invasive tissue sealing. *Adv. Mater.* **2021**, *33*, e2007667.
12 Yuk, H.; Wu, J.; Sarrafian, T. L.; Mao, X.; Varela, C. E.; Roche, E. T.; Griffiths, L. G.; Nabzdyk, C. S.; Zhao, X. Rapid and coagulation-independent haemostatic sealing by a paste inspired by barnacle glue. *Nat. Biomed. Eng.* **2021**, *5*, 1131–1142.
13 Shi, J.; Yu, L.; Ding, J. PEG-based thermosensitive and biodegradable hydrogels. *Acta Biomater.* **2021**, *128*, 42–59.
14 Wang, Y. Q.; Dou, X. Y.; Wang, H. F.; Wang, X.; Wu, D. C. Dendrimer-based hydrogels with controlled drug delivery property for tissue adhesion. *Chinese J. Polym. Sci.* **2021**, *39*, 1421–1430.
15 Xue, B.; Gu, J.; Li, L.; Yu, W.; Yin, S.; Qin, M.; Jiang, Q.; Wang, W.; Cao, Y. Hydrogel tapes for fault-tolerant strong wet adhesion. *Nat. Commun.* **2021**, *12*, 7156.
16 Fichman, G.; Andrews, C.; Patel, N. L.; Schneider, J. P. Antibacterial gel coatings inspired by the cryptic function of a mussel byssal peptide. *Adv. Mater.* **2021**, *33*, e2103677.
17 Liang, Y.; Li, Z.; Huang, Y.; Yu, R.; Guo, B. Dual-dynamic-bond cross-linked antibacterial adhesive hydrogel sealants with on-demand removability for post-wound-closure and infected wound healing. *ACS Nano* **2021**, *15*, 7078–7093.
18 Ma, C.; Sun, J.; Li, B.; Feng, Y.; Sun, Y.; Xiang, L.; Wu, B.; Xiao, L.; Liu, B.; Petrovskii, V. S.; Bin, L.; Zhang, J.; Wang, Z.; Li, H.; Zhang, L.; Li, J.; Wang, F.; Gstl, R.; Potemkin, Il; Chen, D.; Zeng, H.; Zhang, H.; Liu, K.; Herrmann, A. Ultra-strong bio-glue from genetically engineered polypeptides. *Nat. Commun.* **2021**, *12*, 3613.
19 Bevilacqua, M. P.; Huang, D. J.; Wall, B. D.; Lane, S. J.; Edwards, C. K., 3rd; Hanson, J. A.; Benitez, D.; Solomkin, J. S.; Deming, T. J. Amino acid block copolymers with broad antimicrobial activity and barrier properties. *Macromol. Biosci.* **2017**, *17*, 1600492.
20 Xu, W. K.; Tang, J. Y.; Yuan, Z.; Cai, C. Y.; Chen, X. B.; Cui, S. Q.; Liu, P.; Yu, L.; Cai, K. Y.; Ding, J. D. Accelerated cutaneous wound healing using an injectable teicoplanin-loaded PLGA-PEG-PLGA thermogel dressing. *Chinese J. Polym. Sci.* **2019**, *37*, 548–559.
21 Lu, D.; Wang, H.; Li, T. e.; Li, Y.; Wang, X.; Niu, P.; Guo, H.; Sun, S.; Wang, X.; Guan, X.; Ma, H.; Lei, Z. Versatile surgical adhesive and hemostatic materials: synthesis, properties, and application of thermoresponsive polypeptides. *Chem. Mater.* **2017**, *29*, 5493–5503.
22 Li, S.; Chen, N.; Li, X.; Li, Y.; Xie, Z.; Ma, Z.; Zhao, J.; Hou, X.; Yuan, X. Bioinspired double-dynamic-bond crosslinked bioadhesive enables post-wound closure care. *Adv. Funct. Mater.* **2020**, *20*, 2000130.
23 Bonduelle, C.; Lecommandoux, S. Synthetic glycopolypeptides as biomimetic analogues of natural glycoproteins. *Biomacromolecules* **2013**, *14*, 2973–2983.
24 Parani, M.; Lokhande, G.; Singh, A.; Gaharwar, A. K. Engineered nanomaterials for infection control and healing acute and chronic wounds. *ACS Appl. Mater. Interfaces* **2016**, *8*, 10049–10069.
25 Gao, Y.; Li, Z.; Huang, J.; Zhao, M.; Wu, J. *In situ* formation of injectable hydrogels for chronic wound healing. *J. Mater. Chem. B* **2020**, *8*, 8768–8780.
26 Wang, D.; Yang, X.; Liu, Q.; Yu, L.; Ding, J. Enzymatically cross-linked hydrogels based on a linear poly(ethylene glycol) analogue for controlled protein release and 3D cell culture. *J. Mater. Chem. B* **2018**, *6*, 6067–6079.
27 Ren, K.; Li, B.; Xu, Q.; Xiao, C.; He, C.; Li, G.; Chen, X. Enzymatically crosslinked hydrogels based on linear poly(ethylene glycol) polymer: performance and mechanism. *Polym. Chem.* **2017**, *8*, 7017–7024.
28 Zhang, K.; Feng, Q.; Fang, Z.; Gu, L.; Bian, L. Structurally dynamic hydrogels for biomedical applications: pursuing a fine balance between macroscopic stability and microscopic dynamics. *Chem. Rev.* **2021**, *121*, 11149–11193.
29 Poustchi, F.; Amani, H.; Ahmadian, Z.; Niknezhad, S. V.; Mehrabi, S.; Santos, H. A.; Shahbazi, M. A. Combination therapy of killing diseases by injectable hydrogels: from concept to medical applications. *Adv. Healthc. Mater.* **2020**, *10*, 2001571.
30 Guo, B.; Dong, R.; Liang, Y.; Li, M. Haemostatic materials for wound healing applications. *Nat. Rev. Chem.* **2021**, *5*, 773–791.
31 Huang, Y.; Zhao, X.; Zhang, Z.; Liang, Y.; Yin, Z.; Chen, B.; Bai, L.; Han, Y.; Guo, B. Degradable gelatin-based IPN cryogel hemostat for rapidly stopping deep noncompressible hemorrhage and simultaneously improving wound healing. *Chem. Mater.* **2020**, *32*, 6595–6610.
32 Yu, J.; Wang, K.; Fan, C.; Zhao, X.; Gao, J.; Jing, W.; Zhang, X.; Li, J.; Li, Y.; Yang, J.; Liu, W. An ultrasoft self-fused supramolecular polymer hydrogel for completely preventing postoperative tissue adhesion. *Adv. Mater.* **2021**, *33*, 2008395.

33 Cui, C.; Liu, W. Recent advances in wet adhesives: adhesion mechanism, design principle and applications. *Prog. Polym. Sci.* **2021**, *116*, 101388.
34 Maleki, A.; He, J.; Bochani, S.; Nosrati, V.; Shahbazi, M. A.; Guo, B. Multifunctional photoactive hydrogels for wound healing acceleration. *ACS Nano* **2021**, *15*, 18895−18930.
35 Zhang, J.; Zheng, Y.; Lee, J.; Hua, J.; Li, S.; Panchamukhi, A.; Yue, J.; Gou, X.; Xia, Z.; Zhu, L.; Wu, X. A pulsatile release platform based on photo-induced imine-crosslinking hydrogel promotes scarless wound healing. *Nat. Commun.* **2021**, *12*, 1670.
36 Xu, X.; Xia, X.; Zhang, K.; Rai, A.; Li, Z.; Zhao, P.; Wei, K.; Zou, L.; Yang, B.; Wong, W. K.; Chiu, P. W. Y.; Bian, L. Bioadhesive hydrogels demonstrating pH-independent and ultrafast gelation promote gastric ulcer healing in pigs. *Sci. Trans. Med.* **2020**, *12*, eaba8014.
37 Ahmadian, Z.; Correia, A.; Hasany, M.; Figueiredo, P.; Dobakhti, F.; Eskandari, M. R.; Hosseini, S. H.; Abiri, R.; Khorshid, S.; Hirvonen, J.; Santos, H. A.; Shahbazi, M. A. A hydrogen-bonded extracellular matrix-mimicking bactericidal hydrogel with radical scavenging and hemostatic function for pH-responsive wound healing acceleration. *Adv. Healthc. Mater.* **2020**, *10*, 2001122.
38 Arno, M. C. Engineering the mammalian cell surface with synthetic polymers: strategies and applications. *Macromol. Rapid Commun.* **2020**, *41*, 2000302.
39 Xu, C.; Yu, B.; Qi, Y.; Zhao, N.; Xu, F. J. Versatile types of cyclodextrin-based nucleic acid delivery systems. *Adv. Healthc. Mater.* **2020**, *10*, 2001183.
40 Cheng, Y.; Zhao, L.; Li, Y.; Xu, T. Design of biocompatible dendrimers for cancer diagnosis and therapy: current status and future perspectives. *Chem. Soc. Rev.* **2011**, *40*, 2673.
41 Liu, C.; Liu, X.; Liu, C.; Wang, N.; Chen, H.; Yao, W.; Sun, G.; Song, Q.; Qiao, W. A highly efficient, *in situ* wet-adhesive dextran derivative sponge for rapid hemostasis. *Biomaterials* **2019**, *205*, 23−37.

https://doi.org/10.1007/s10118-022-2741-1